Catal Lett (2007) 118:139–145
DOI 10.1007/s10562-007-9170-1

Production of CO_X Free Hydrogen by Catalytic Decomposition of Methane Over Ni/HY Catalysts

Jangam Ashok · Sathu Naveen Kumar · Machiraju Subrahmanyam · Akula Venugopal

Received: 18 May 2007 / Accepted: 14 June 2007 / Published online: 14 July 2007

Abstract In this present paper, we report catalytic decomposition of methane over Ni/HY catalysts, with varying Ni loading at 550 °C and atmospheric pressure. The relationships between catalyst performance and characterization of the fresh and used form of catalysts are discussed from the data obtained by scanning electron microscopy, X-ray diffraction analysis, temperature programmed reduction, O_2 pulse chemisorption and carbon elemental analyses. It is observed that, the catalytic activity of Ni/HY catalysts is high at initial stages and gradually decreased with time and finally deactivated completely. The yield of hydrogen and carbon nanofibers is strongly dependent on Ni loading. It is found that 20 wt% Ni/HY catalyst showed higher hydrogen yield over the other loadings.

Keywords Nickel · Hydrogen production · Carbon nanofibers · HY zeolite · Methane decomposition · O_2 pulse chemisorption

1 Introduction

Hydrogen is the most suitable fuel particularly for fuel cell applications. The available methods for H_2 production are steam reforming, partial oxidation and auto-thermal reforming of hydrocarbons. However, a major drawback is associated with these routes is the formation of large amount of CO_x as byproducts along with hydrogen. Hydrogen generated by these conventional methods can be utilized in fuel cells only if CO is completely eliminated [1]. The problem associated with CO in H_2 stream can be avoided by catalytic decomposition of methane. The catalytic decomposition of methane (CDM) over Ni based catalysts is extensively studied systems due to the growing importance on the production of pure H_2 as well as the formation of useful compounds such as carbon nanotubes (CNT) and carbon nanofibers (CNF) [2–6]. On economical perspective the H_2 production rate and the CNF or CNT synthesis are equally important. Due to unique properties of the CNTs and CNFs [2, 7] they are emerged as potential components in various applications such as catalyst supports [8–10], hydrogen storage materials [11], electronic and mechanical devices [12], composite materials [13] and adsorption/absorption agents [14]. Choudhary et al. have studied the nature and type of carbon formed during methane decomposition over Ni based catalysts [15]. Ermakova et al. have studied the effect of method of preparation, nature of support material and the influence of textural promoters on Ni catalysts [3, 16]. The important factor that would influence the carbon yield during methane decomposition is the amount of nickel, Ni particle size, Ni dispersion and stabilization of the metallic nickel particles that can be tuned by selecting appropriate support [17]. Earlier we have examined the effect of catalyst supports namely SiO_2, SBA-15, USY, HY, HAp for Ni on the catalytic activity for methane decomposition and reported that HY zeolite is one of the promising support material for the decomposition of methane to form hydrogen and carbon nanofibers [18–20]. Thus, we focused our attention on various Ni loaded HY catalysts. The present study deals with CDM activities and the correlation between physico-chemical characteristics of the fresh and used form of catalysts obtained by SEM, XRD, TPR, O_2 pulse chemisorption and

J. Ashok · S. Naveen Kumar · M. Subrahmanyam · A. Venugopal (✉)
Catalysis and Physical Chemistry Division, Indian Institute of Chemical Technology, Hyderabad 500 007, India
e-mail: akula@iict.res.in

CHNS analyses. The methane decomposition activities were measured at 550 °C and atmospheric pressure.

2 Exprimental

Ni/HY was prepared by impregnating (surface area = 500 m^2/g, Si/Al = 2.6, supplied by P Q Corporation) nickel nitrate [Ni $(NO_3)_2 \cdot 6H_2O$] solution on HY zeolite. In a typical method required amount of nickel nitrate is taken to give various Ni loading catalysts of 10, 15, 20, 25, 30, 40, 50 and 60 wt% with known amount of water in a 100 ml beaker and mixed with the requisite amounts of HY zeolite to yield the respective Ni mass percentages as mentioned above, followed by a drying up the impregnated sample at 100 °C for 24 h and subsequently calcined in air at 700 °C for 5 h. Thus prepared catalysts are called as fresh catalysts, which are used for evaluation of CDM reaction.

The SEM images of the fresh and used catalysts were recorded using a JEOL-JSM 5600 instrument. X-Ray Diffraction (XRD) patterns of all the samples are obtained on a Rigaku miniflex X-ray diffractometer using Ni filtered Cu K_α radiation (λ = 1.5406 Å) from 2θ = 2–80° at a scan rate of 2° min^{-1} with the beam voltage and a beam current of 30 kV and 15 mA respectively. The nickel crystallite size is estimated using Scherrer equation [21]. Temperature Programmed Reduction (TPR) and O_2 chemisorption analysis were carried out using a pulse micro reactor inter faced to GC with thermal conductivity detector. For TPR analysis the catalyst sample of about 50 mg was loaded in an isothermal zone of a quartz reactor (i.d = 6 mm, length = 300 mm) heated by an electric furnace and heated at a rate of 10 °C/min to 450 °C in 30 cc/min helium gas, which facilitates to desorb physically adsorbed water. After the sample was cooled to room temperature, the helium gas was replaced with 5% H_2/Ar at a flow rate of 20 cc/min and the temperature was increased to 700°C at a ramping rate of 5°C/min. Hydrogen consumption was measured by analyzing effluent gas by means of Thermal Conductivity Detector (TCD). The steam formed during reduction was removed by molecular sieve trap. After TPR analysis the same sample was cooled to 430 °C in helium gas, out gassed at this temperature for 30 min, followed by titration with 5.01% O_2 in helium gas at 430 °C. The O_2 uptakes were calculated assuming the formation of NiO phase [22]. The carbon analysis data was collected with VARIO EL CHNS analyser.

The catalytic activities are performed at 550 °C in atmospheric pressure in a fixed-bed vertical quartz reactor (i.d = 20 mm, length = 460 mm), operated in a down flow mode heated by an electric furnace. Methane supplied by Vadilal gases limited (99.99%) is used directly without further purification. Helium is used as a diluent gas. The experimental conditions used are as reported earlier [18, 23] and some of the details are provided as; catalyst charge of 50 mg, methane flow rate = 20 cc/min, helium flow rate = 40 cc/min i.e., GHSV of 72.0 L (h g-cat)$^{-1}$. Prior to the reaction, the catalyst is reduced at 450 °C with 5% H_2 in N_2 for 2 h. The methane gas is passed through pre-heating zone, which is maintained at 200 °C. The reaction was continued until the catalysts are completely deactivated. The outflow gas was analyzed by Varian Gas Chromatography Model No. 3800 equipped with a carbosphere column and TCD detector using N_2 as a carrier gas. The concentrations of methane and hydrogen in the product stream were calculated using calibrated data and then methane conversion (defined as number of moles of methane converted by number of moles of methane fed in) was calculated. The first analysis was done 5 min after methane was fed over the catalyst. An experimental error of the order of ±5 in activity evaluation studies was noted during the evaluation.

3 Result and Discussion

3.1 Catalyst Performance Evaluation

Figure 1 shows changes in methane conversion (%) as a function of time (min) during the catalytic decomposition of methane at 550 °C over Ni/HY catalysts with different loadings of Ni (Ni wt% were varied from 10 to 60). The activity measurements were carried out under similar reaction conditions until complete deactivation of the catalyst, in order to examine the influence of Ni loadings on HY zeolite. Carbon and hydrogen were the only products observed in this study [18, 19]. It is clear from Fig. 1 that methane conversion is found to be high in the initial stages and decreased rapidly or gradually with time on stream as a

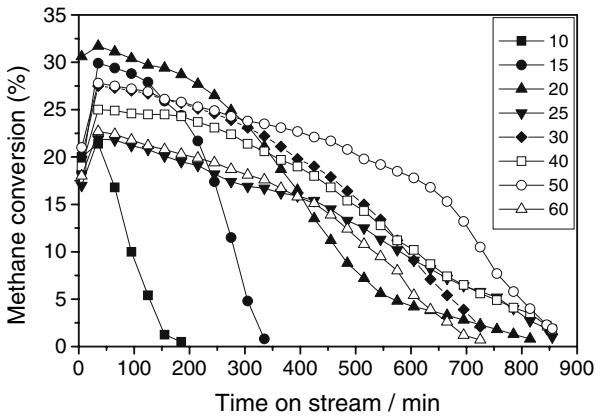

Fig. 1 Methane conversions (%) with time (min) over Ni/HY catalysts at 550 °C temperature

result of carbon deposition. Finally, all the catalysts were deactivated completely over a period of time. The catalyst deactivation is attributed due to the deposition of carbon on the catalyst surface/active sites or accumulated at the entrance of the pores due to pore blockage. The reaction run time until complete deactivation of the catalysts are increased in the order 10 < 15 < 60 < 30 < 20 < 25 ~ 40 < 50 wt% of Ni over HY zeolite. The typical volcano-shape relationship obtained (Fig. 2) with carbon formed per mole of nickel (C/Ni) of the catalyst with Ni loading, indicate how critical is the role of the metal quantity on the catalyst performance during the CDM reaction. The theoretical stoichiometry carbon yields were denoted as C/Ni (moles of carbon deposited per mole of nickel) and this corresponds to half of H_2/Ni mole ratio. The carbon yields were estimated from the kinetic curves of methane conversion and they were shown in Fig. 1. The C/Ni values are increased in the order of 60 < 10 < 50 < 40 < 30 < 25 < 15 < 20 wt% Ni/HY. We have earlier observed the similar volcano type of tendency of H_2 yields over Ni/SiO_2 catalysts during the catalytic decomposition of methane [19]. The catalyst deactivation and the carbon fibers growth rates depend upon several factors like diffusion flux area, diffusion length, driving force of carbon diffusion and saturation concentration of carbon nanofibers [24]. The average Ni crystallite size for Ni/HY catalysts was calculated using Scherrer formula from the XRD patterns and the corresponding values are reported in Table 1. It is clear that the crystallite size of Ni is increased with increasing Ni loading. The increase in the size of Ni crystal is due to the agglomeration of Ni particles during preparation. De Chen et al. observed that low coking rate on small size Ni crystal is a result of increased saturation concentration of carbon fibers which leads to a low driving force of carbon diffusion and then a lower coking rate eventually causes drastic deactivation of the catalyst, on the contrary over large Ni particles, the formation of surface carbon from elementary reaction steps could become the rate determining step [25]. Thus suggesting the fundamental role in the kinetics of coke formation with respect to Ni particle size which otherwise is dependent on the loading. In the present study the 20 wt% Ni/HY catalyst with an average crystallite size of 15 nm displayed a high hydrogen yield of 1,355 mol H_2/mol Ni.

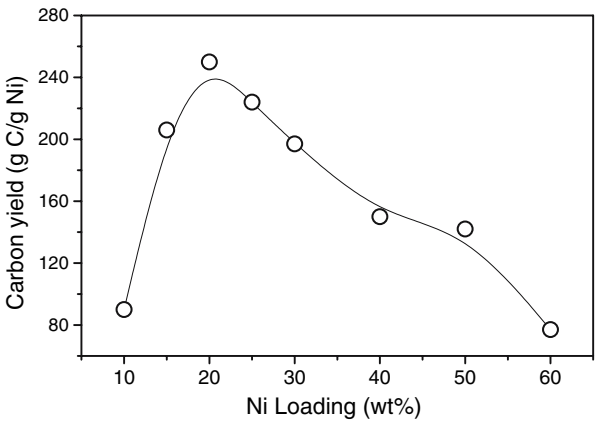

Fig. 2 Carbon yields during methane decomposition as a function of Ni loading over Ni/HY catalysts

3.2 Powder X-ray Diffraction (XRD) Analysis

The powder XRD patterns of fresh and deactivated Ni/HY catalysts were shown in Figs. 3 and 4 respectively. The appearance of reflections (Fig. 3) at 2θ = 6.17°, 10.0°, 11.8° and 15.5° and their corresponding 'd' values, 14.29, 8.75, 7.46 and 5.67 Å are attributed due to the presence of a HY zeolite phase **[ICDS # 74-1192]**. However the intensity of HY phase is decreased with increasing Ni loading. Figure 4, indicates the reflections at 2θ = 37.28°, 43.3°, 62.9° and their corresponding 'd' values, 2.09, 1.48, 2.41 Å are pertaining to the presence of crystalline NiO phase **[ICDS # 01-1239]**. However the NiO phase is not so clear at lower loadings but is dominated in higher nickel loadings. The NiO phase in the fresh catalysts suggest the decomposition of nickel nitrate in air at 700 °C for 5 h to form the NiO species during the preparation and calcination of catalysts. It is clearly observed from the XRD patterns (Fig. 3) that the intensity of NiO phase is increased with increase in Ni loading. Figure 4 reveals the diffraction lines at 2θ = 26.28°, 45.2°, 53.9° and 77.0° and their corresponding 'd' values of 3.38, 2.00, 1.69 and 1.23 Å are attributed to graphitic carbon **[ICDS # 01-0640]** as well as the phase due to metallic Ni reflections at 2θ = 44.4°, 51.8° and 76.4° and the corresponding 'd' values 2.03, 1.76, 1.24 Å in the deactivated form of catalysts **[ICDS # 04-0850]**. It is also observed that decrease in peak intensities of HY phase in the deactivated catalysts with increase in Ni loadings. Thus concludes the XRD analysis revealed NiO, HY phases in fresh and metallic Ni, graphitic carbon and HY phases in deactivated form of the catalysts.

3.3 Temperature Programmed Reduction (TPR)

The objective of TPR experiments was to determine the reducibility as well as the T_{max} of the catalysts. TPR may be used to determine the location of Ni^{2+} sites within the zeolite with the relative ease of Ni^{2+} reduction decreasing in the order: supercages > sodalite cages > hexagonal prisms [26]. The TPR profiles of all the catalysts calcined at 700 °C reported in Fig. 5 and the H_2 uptakes are given in Table 1. The H_2 uptakes were linearly increased with Ni loading suggests the bulk property of H_2-TPR. The XRD analysis (Fig. 3) of the fresh catalysts also revealed that the NiO

Table 1 Physico-chemical characteristics of the Ni/HY catalysts

Ni (wt%)	[a]Ni Crystallite size (nm)	[b]H_2 uptakes (mmols/g)	[c]O_2 uptakes (μmol/g)	S_{Ni} (m^2/g)	[d]H_2 yields (mol H_2/mol Ni)	[e]Carbon yields (gC/g–Ni)
10	12	1.5	4.32	0.23	440	90
15	13	2.2	5.15	0.27	993	206
20	15	3.0	7.51	0.400	1355	250
25	16	3.9	7.25	0.386	970	224
30	18	4.6	7.05	0.375	955	197
40	22	6.3	6.82	0.363	712	150
50	25	8.1	6.80	0.362	704	142
60	29	9.2	6.63	0.353	370	77

[a] From XRD analysis

[b] From TPR

[c] From O_2 pulse chemisorption

[d] From CDM activities

[e] From CHNS analysis

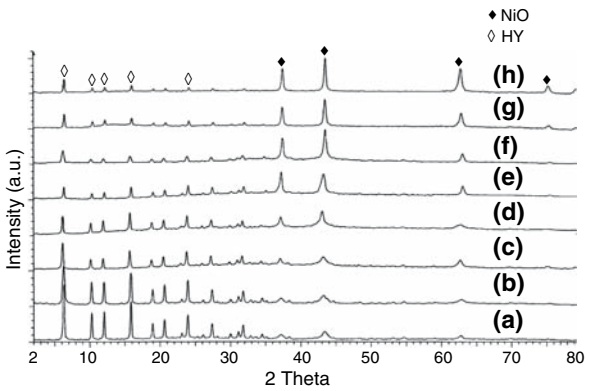

Fig. 3 XRD patterns of fresh (a) 10, (b) 15, (c) 20, (d) 25, (e) 30, (f) 40, (g) 50 and (h) 60 wt% Ni over HY zeolite

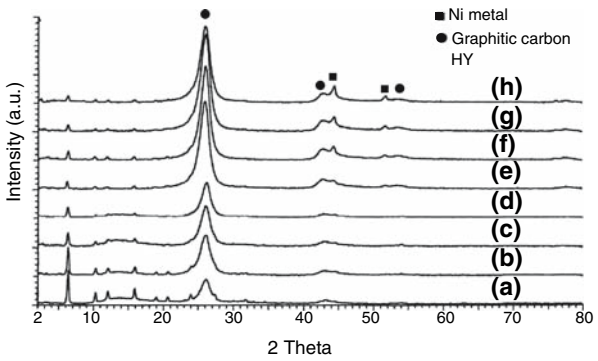

Fig. 4 XRD patterns of used (a) 10, (b) 15, (c) 20, (d) 25, (e) 30, (f) 40, (g) 50 and (h) 60 wt% Ni over HY zeolite

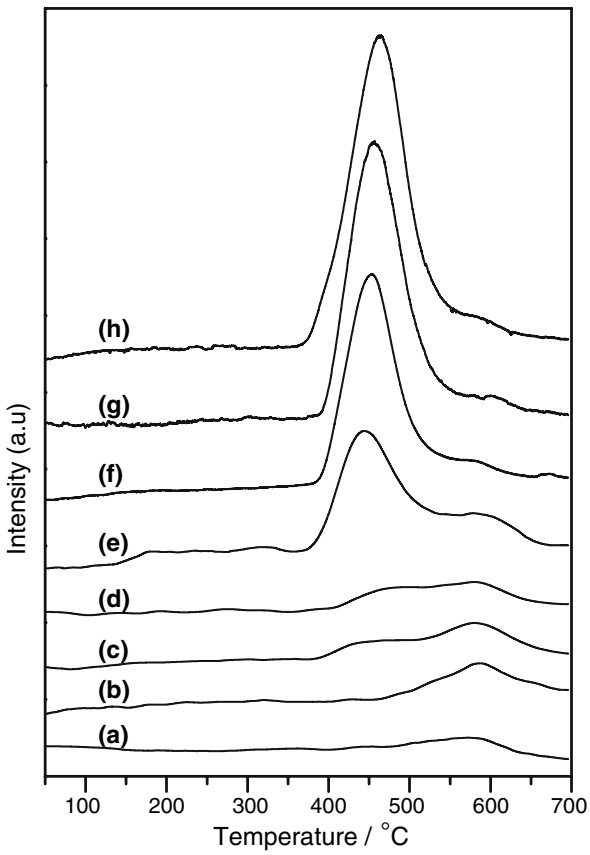

Fig. 5 TPR profiles of (a) 10, (b) 15, (c) 20, (d) 25, (e) 30, (f) 40, (g) 50 and (h) 60 wt% Ni loaded over HY zeolite

peak intensities were increased with nickel loadings. Figure 5 shows two stage reduction, a low temperature reduction peak centered at ~450 °C and a high temperature reduction peak centered at ~600 °C at and above 20 wt% Ni loaded catalysts. Where as a single high temperature reduction peak is observed only in case of 10, 15 wt% Ni/HY catalysts. The low temperature reduction peak ~450 °C

can be attributed to reduction of NiO particles located at the outer surface of the zeolite crystals and the high temperature peak centered ~600 °C is assigned to reduction of Ni^{2+} in sodalite cages to Ni° and Ni^{1+} as observed Hurst et al. over NiNaX zeolite catalysts [27]. From relative peak areas, it is clear that the intensity of high temperature reduction peak (~600 °C) is almost same irrespective of Ni loading, where as the H_2 consumption for low temperature peak (~450 °C) is increased with increasing Ni loading. It is concluded that reduction peaks at 450 °C and 600 °C are due to the reduction of NiO species that are located at outer surface and sodalite cages of zeolite crystals respectively. With increase in nickel loading the low temperature reduction peak intensities increased thus suggests the formation of large size NiO particles at the outer surface of the zeolite.

3.4 O_2 Pulse Chemisorption Measurements

The O_2 uptakes for Ni/HY catalysts were measured using O_2 pulse chemisorption method as reported earlier [20] and results were reported in Table 1. The Ni metal surface area was calculated using O_2 uptakes and plotted against H_2 production yields over Ni/HY catalysts. It is clear from Fig. 6, a linear relationship is observed between the Ni metal surface area and the H_2 yields obtained from CDM reaction. Thus it is concluded that the H_2 production rate is dependent up on the amount of Ni metal surface area of Ni/HY catalysts.

3.5 SEM Analysis

The SEM micrographs of fresh and used Ni/HY catalysts were shown in Fig. 7. The images are measured before and after (complete deactivation) the methane decomposition activity carried out at 550 °C over the Ni/HY catalysts with Ni loading amounts of 10, 20, and 50 wt%. It is seen that

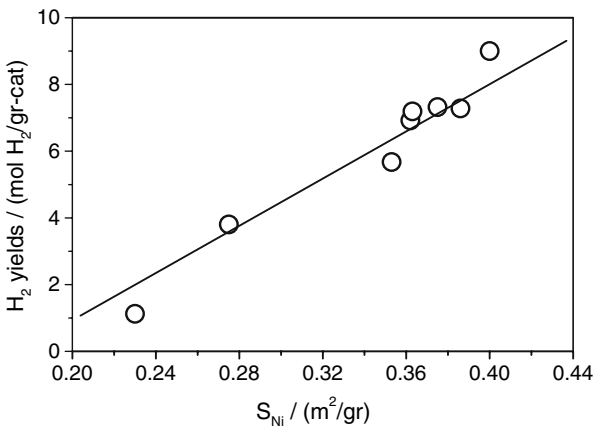

Fig. 6 Hydrogen yields as a function of surface area of Ni over Ni/HY catalysts

deposited carbon over all the catalysts are whisker type nano filament ones. However the diameter and lengths of the carbon nanofilaments are different. The yield of carbon nano fiber strongly depends on the Ni particle size and the support plays a key role on the nature of type carbon formed [15]. The Ni metal particle that decomposed the methane to grow carbon nanofiber (CNF) is found to be graphitic carbon as evidenced from the XRD analysis of the deactivated catalyst. The whisker type of CNF is an indication of high catalytic activity and a long lifetime during methane decomposition over oxidized diamond supported Ni catalysts [28]. Choudhary et al. observed the filamentous carbon during methane decomposition over Ni/HY and Ni/SiO_2 catalysts [29]. It appears that the nature and type of carbon formed would also dependent upon the source of carbon used. Zhou et al. reported that platelet CNFs are obtained using Fe powder as catalyst and CO as carbon source, fishbone CNF over alumina supported Ni–Fe alloy catalyst in presence of CO, CH_4 and/or C_2H_4 as carbon source and tubular CNF over alumina supported Ni catalyst and CO as carbon source. However, the structural and textural properties of the CNFs seems to be varied in a wide range [30]. In the present study the Ni/HY deactivated catalysts displayed CNF that are whisker in nature. The low catalytic activity is due to rapid carbon deposition on the catalyst active sites. The SEM images of deactivated catalysts (Fig. 7) distinguished the bright spots attributed to the Ni particles appeared at the tip of CNF that are more abundant over 20 wt% Ni compared to 10 and 50 wt% Ni/HY catalysts.

3.6 Carbon Elemental Analysis

All the deactivated catalysts were recovered in an inert gas and subsequently estimated for the carbon contents by CHNS analyses. The XRD analysis of the deactivated catalysts revealed the presence of graphitic carbon. The activity of the catalyst can be correlated from the carbon estimations of the deactivated catalysts obtained after CDM reaction. The amount of carbon deposition is found to be high over 20 wt% Ni/HY compared to other catalysts. The irreversibility of the reaction is further confirmed by the TPR analysis of the deactivated catalyst, which could not display any reduction profile due to hydrogasification, i.e. carbon hydrogenation even upto 750 °C.

4 Conclusions

The physicochemical properties of the catalysts were characterized using SEM, XRD, TPR,O_2 pulse chemisorption and carbon elemental analysis and correlated with methane decomposition activity. The following observa-

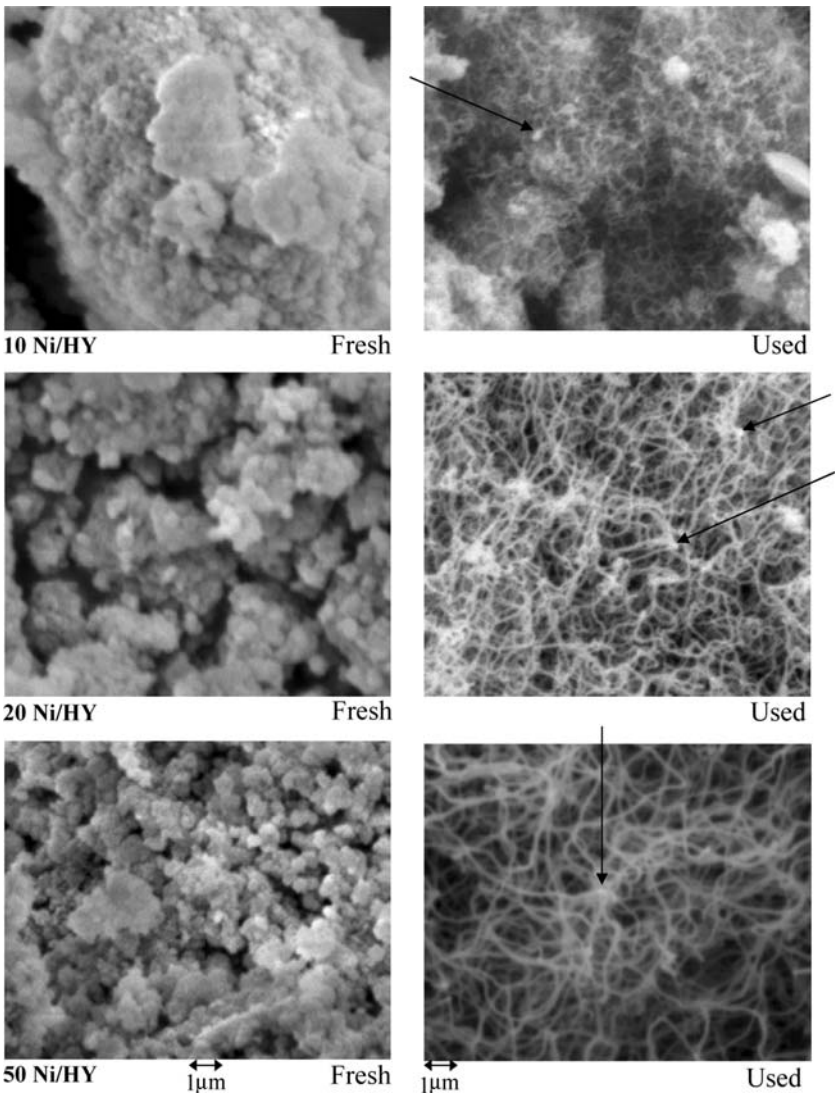

Fig. 7 The SEM images of fresh and used 10, 20, 50 wt% Ni/HY catalysts

tions were made based on the results obtained. Powder XRD analysis revealed the presence of NiO and HY zeolite phases in fresh form and metallic Ni, graphitic carbon and HY zeolite phases in the deactivated catalysts. The TPR studies emphasized two stages reduction at and above 20 wt% Ni/HY catalysts. The SEM images of deactivated catalysts displayed carbon nanofibers and the bright spots appeared at the tip of the nanofiber. The 20 wt% Ni/HY catalyst showed higher activity than the other nickel loadings, which is explained based on the Ni metal surface area obtained by O_2 pulse chemisorption studies.

Acknowledgments The authors thank CSIR, New Delhi for funding this project under NMITLI program.

References

1. Choudhary TV, Goodman DW (2002) Catal Today 77:65
2. De Jong KP, Geus JW (2000) Catal Rev Sci Eng 42:481
3. Ermakova MA, Ermakov DY, Kuvshinov GG (2000) Appl Catal A 201:61
4. Colomer JF, Stephan C, Lefrant S, Van Tendeloo G, Willems I, Konya Z, Fonseca A, Laurent C, Nagy JB (2000) Chem Phys Lett 317:83
5. Villacampa JI, Royo C, Romeo E, Montoya JA, Del Angel P, Monzón A (2003) Appl Catal A 252:363
6. Chen D, Lodeng R, Holmen A (1999) Stud Surf Sci Catal 126:473
7. Ebbesen TW (1997) Carbon nanotubes: preparation and properties. CAPLUS, USA
8. Rodriguez NM, Kim MS, Baker RTK (1994) J Phys Chem 98:13108
9. Bahome MC, Jewell LL, Hildebrandt D, Glasser D, Coville NJ (2005) Appl Catal A 287:60
10. Serp P, Corrias M, Kalck P (2003) Appl Catal A 253:337
11. Chambers A, Park C, Baker RTK, Rodriguez NM (1998) J Phys Chem B 102:4253
12. Dai H, Hafner JH, Rinzler AG, Colbert DT, Smalley RE (1996) Nature 384:147
13. Lozano K, Barrera EV (2000) J Appl Polym Sci 79:125
14. Park C, Engel ES, Crowe A, Gilbert TR, Rodriguez NM (2000) Langmuir 16:8050

15. Choudhary TV, Aksoylu E, Goodman DW (2003) Catal Rev 45:151
16. Ermakova MA, Ermakov DY, Kuvshinov GG, Plyasova LM (1999) J Catal 187:77
17. Rostrup-Nielsen JR (1975) Teknisk Forlag A/S, Copenhagen
18. Ashok J, Naveen Kumar S, Venugopal A, Durga Kumari V, Subrahmanyam M (2007) J Power Sources 164:805
19. Venugopal A, Ashok J, Naveen kumar S, Durga Kumari V, Prasad KBS, Subrahmanyam M (2007) Int J Hydrogen Energy 2007, (Available on-line 26th February 2007)
20. Venugopal A, Ashok J, Naveen kumar S, Durga Kumari V, Subrahmanyam M (2007) Manuscript submitted to Catal Comm
21. Bond GC (1987) Heterogeneous catalysis: principles and applications. Oxford University Press, New York, p 81
22. Stytsenko VD (1995) Appl Catal A 126:1
23. Ashok J, Naveen Kumar S, Venugopal A, Durga Kumari V, Tripathi S, Subrahmanyam M (2007) Catal Comm (Accepted for publication)
24. Bonura G, Di Blasi O, Spadaro L, Arena F, Frusteri F (2006) Catal Today 116:298
25. Chen D, Christensen KO, Fernández EO, Yu Z, Totdal B, Latorre N, Monzon A, Holmen A (2005) J Catal 229:82
26. Homeyer ST, Sachtler WMH (1989) J Catal 117:91
27. Hurst NW, Gentry SJ, JonesA, McNicol BD (1982) Catal Rev Sci Eng 24:233
28. Nakagawa K, Gamo MN, Ando T (2005) Int J Hydrogen Energy 30:201
29. Choudhary TV, Sivadinarayana C, Chusuei CC, Klinghoffer A, Goodman DW (2001) J Catal 199:9
30. Zhou JH, Sui ZJ, Li P, Chen D, Dai YC, Yuan WK (2006) Carbon 44:3255